

Decoupled energy-law preserving numerical schemes for the Cahn-Hilliard-Darcy system

Daozhi Han, Xiaoming Wang

Department of Mathematics

Florida State University

Tallahassee, Florida, 32306

We study two novel decoupled energy-law preserving numerical schemes for solving the Cahn-Hilliard-Darcy (CHD) system which models two-phase flow in porous medium or in a Hele-Shaw cell. In the first scheme, the velocity in the Cahn-Hilliard equation is treated explicitly so that the Darcy equation is completely decoupled from the Cahn-Hilliard equation. In the second scheme, an intermediate velocity is employed in the Cahn-Hilliard equation which allows for the decoupling. We show that the first scheme preserves a discrete energy law with a time-step constraint, while the second scheme satisfies an energy law without any constraint and is unconditionally stable. Ample numerical experiments are performed to gauge the efficiency and robustness of our scheme. © (Year) John Wiley & Sons, Inc.

Keywords: Cahn-Hilliard-Darcy; two-phase flow; porous medium; Hele-Shaw cell; decoupling; stability; long-time stability; energy-law; convex-splitting

I. INTRODUCTION

In the present contribution, we consider solving numerically the Cahn-Hilliard-Darcy (CHD) system which is a diffuse interface model for two-phase incompressible flow in

porous medium or a Hele-Shaw cell. The model in dimensionless form is given as follows

$$\frac{ReDa}{\chi} \frac{\partial \mathbf{u}}{\partial t} + \alpha(\phi) \mathbf{u} = -\nabla p - \frac{\epsilon^{-1}}{We^*} \phi \nabla \mu, \quad (1.1)$$

$$\nabla \cdot \mathbf{u} = 0, \quad (1.2)$$

$$\chi \frac{\partial \phi}{\partial t} + \nabla \cdot (\phi \mathbf{u}) = \frac{1}{Pe} \nabla \cdot (m(\phi) \nabla \mu), \quad (1.3)$$

$$\mu = \phi^3 - \phi - \epsilon^2 \Delta \phi, \quad (1.4)$$

where Re is the Reynolds number, Da is the Darcy number (a measure of the permeability relative to the area of the domain), χ is the porosity, We^* is the modified Weber number (a measure of kinetic energy vs surface energy), ϵ is a constant representing the non-dimensionalized thickness of the transition layer between the two phases, Pe is the diffusional Peclet number measuring the importance of advection over diffusion, and m is the dimensionless mobility. Here $\alpha(\phi)$ is the reciprocal of the dimensionless hydraulic conductivity defined as $\alpha(\phi) = \frac{\eta(\phi)}{\Pi}$ with $\eta(\phi)$ the dimensionless viscosity coefficient and Π the dimensionless permeability. Throughout, we assume $\alpha(\phi)$ and $m(\phi)$ are bounded below and above, i.e.,

$$0 < \alpha_1 \leq \alpha(\phi) \leq \alpha_2, \quad 0 < m_1 \leq m(\phi) \leq m_2. \quad (1.5)$$

The Eqs. (1.1) and (1.2) are the Darcy system with time derivative retained for flow in porous medium [3, 30]. \mathbf{u} is the nondimensionalized seepage velocity and p is the non-dimensionalized modified pressure [24]. The last two Eqs. (1.3) and (1.4) are the Cahn-Hilliard equation written as a system of two second order equations. ϕ is the non-dimensionalized order parameter/phase field variable which takes values $\{1\}$ and $\{-1\}$ in the pure fluids and vary continuously across the transition layer between the two fluids. μ is the dimensionless chemical potential. Note that the Reynolds number and Darcy number are typically small for flow in porous medium. Formally setting $Da = 0$ in Eq. (1.1), one recovers the standard Cahn-Hilliard-Hele-Shaw/Darcy system studied by many authors [24, 25, 39, 38, 37, 26, 21]. The current version of the CHD model is heuristically more accurate than the standard one as the non-stationary effect is neglected in the static Darcy equation, cf. [16, 5].

We close the system with the following initial and boundary conditions

$$\mathbf{u}|_{t=0} = \mathbf{u}_0, \quad (1.6)$$

$$\phi|_{t=0} = \phi_0, \quad (1.7)$$

$$\partial_{\mathbf{n}}\phi|_{\partial\Omega} = 0, \quad (1.8)$$

$$\partial_{\mathbf{n}}\mu|_{\partial\Omega} = 0, \quad (1.9)$$

$$\mathbf{u} \cdot \mathbf{n}|_{\partial\Omega} = 0. \quad (1.10)$$

Here \mathbf{n} is the unit outer normal of the boundary $\partial\Omega$; Eq. (1.8) is a Neumann boundary condition for phase field variable; Eq. (1.9) means that there is no chemical flux through the boundary; Eq. (1.10) is the usual no penetration boundary condition for fluid velocity. With boundary conditions (1.8)-(1.10), it is clear that the CHD system is energy dissipative according to the following energy law

$$\frac{dE}{dt} = -\frac{\epsilon^{-1}}{We^*Pe} \int_{\Omega} m(\phi)|\nabla\mu|^2 dx - \int_{\Omega} \alpha(\phi)|\mathbf{u}|^2 dx \leq 0, \quad (1.11)$$

where E is the total energy

$$E = ReDa \int_{\Omega} \frac{1}{2\chi} |\mathbf{u}|^2 dx + \frac{1}{We^*} \int_{\Omega} \chi \left[\frac{1}{\epsilon} F(\phi) + \frac{\epsilon}{2} |\nabla\phi|^2 \right] dx. \quad (1.12)$$

The first integral in Eq. (1.12) is the kinetic energy, and the second one represents the total free energy with the homogeneous free energy density function $F(\phi) = \frac{1}{4}(\phi^2 - 1)^2$.

The main purpose of this work is to design efficient and stable numerical algorithms for solving the CHD system (1.1)–(1.4). We note that the interfacial thickness ϵ in the system is typically small for macroscopically immiscible binary fluids [2, 27, 28]. Thus the CHD Eqs. represent a coupled nonlinear system that describes physical phenomena of steep spatial variation within a small transition region. Energy-law preserving schemes are preferred for solving such systems for a number of reasons. On one hand, the preservation of the energy law (1.11) is essential for the numerical scheme to capture the correct long time dynamics of the system. On the other hand, the inherent stability from energy law preserving schemes would allow for relatively larger time stepping for solving such a stiff problem [31]. A key idea in the development of energy-law preserving schemes for systems of variational structure is convex splitting (see [8, 39, 36, 20, 32, 15] among many others). Indeed, the convex splitting idea has already been applied to the standard Cahn-Hilliard-

Darcy model [39], Cahn-Hilliard-Stokes model [6] and Cahn-Hilliard-Navier-Stokes model [22, 33, 11, 13, 17] to generate unconditionally stable (with discrete energy law) schemes. The idea of convex-splitting will be one of the key components in the design of our numerical schemes as well.

Despite the abundance of the literature on coupled energy law preserving numerical schemes for phase field fluid models, the work on decoupled schemes are few. In this work, we propose and compare two decoupled energy-law preserving numerical schemes for solving the CHD system. In the first scheme Eqs. (2.11)-(2.13), the decoupling is realized through treating the velocity in the Cahn-Hilliard equation explicitly. Such an idea has been used by many practitioners in the actual computation of Cahn-Hilliard fluid models as well as other advection-diffusion problems. The rationale is that the velocity appears as a low-order term ($\mathbf{u} \cdot \nabla \phi$) in the Cahn-Hilliard equation and is not supposed to contribute to a severe CFL-like condition, cf. [31]. We show that the first scheme indeed satisfies a discrete energy law with a mild time-step constraint. Our first scheme is inspired by [22] where a similar result for the Cahn-Hilliard-Navier-Stokes model was derived. In the second numerical scheme (2.14)-(2.16), we take a fractional stepping approach to decouple the computation of Cahn-Hilliard equation and fluid equation. Following the work of Minjeaud [29] (see also [14]), we employ an intermediate velocity (cf. (2.17)) defined only through the Korteweg force $\frac{\epsilon^{-1}}{We^*} \phi \nabla \mu$ in the Cahn-Hilliard equation. We show that the scheme satisfies an energy law free of time step constraint. Recently, this fractional stepping idea has been generalized to solving Cahn-Hilliard-Navier-Stokes type of systems in various contexts, cf. [34, 35].

There are several unconditionally stable but coupled numerical schemes for solving the standard CHD system without explicit time derivative in Eq. (1.1). In [39], Wise proposes an unconditionally stable finite difference, nonlinear multigrid numerical scheme. Owing to the convex-splitting discretization of the chemical potential equation and implicit treatment of the pressure for the advective velocity in the Cahn-Hilliard equation, he is able to show the unconditionally unique solvability and unconditional stability of his numerical scheme. The same time discretization in conjunction with the local discontinuous Galerkin method is employed by Guo et al. in [12]. The energy stability of their scheme is also established. We refer to [6] for a similar scheme for solving the

Cahn-Hilliard-Brinkman system. Though the energy stability is preserved in all these schemes, one has to solve the nonlinear system in a coupled fashion. In [14], Han designs a decoupled unconditionally stable scheme by combining fractional stepping and pressure stabilization. But the scheme only satisfies a modified energy law with the addition of pressure gradient in the definition of the discrete energy functional. Nonetheless, the scheme is more efficient in theory than the coupled schemes thanks to the decoupling.

The remainder of the paper is structured as follows. In section II., we first present the definition of weak formulation for the CHD system. We then introduce the two numerical schemes for solving the CHD system. We show that both schemes satisfy discrete energy laws at the end of section II.. Some numerical results are presented in section III. to gauge the accuracy, stability and effectiveness in capturing topological changes of the numerical schemes.

II. THE NUMERICAL SCHEME

A. The weak formulation

We formulate the CHD system (1.1)-(1.4) under the boundary conditions (1.8)- (1.10) in a weak form. To this, we introduce the following Hilbert spaces

$$\mathbf{X} = \mathbf{L}^2(\Omega), \quad M = L_0^2(\Omega) = \{q \in L^2(\Omega), \int_{\Omega} q = 0\}, \quad (2.1)$$

$$\mathbf{H} = \{\mathbf{v} \in \mathbf{L}^2(\Omega), \nabla \cdot \mathbf{v} = 0, \mathbf{v} \cdot \mathbf{n}|_{\partial\Omega} = 0\}, \quad (2.2)$$

$$Y = H^1(\Omega). \quad (2.3)$$

A weak formulation and solutions to the initial-boundary value problem (1.1)–(1.10) can be defined similarly as [9].

Definition. *Let $\phi_0 \in Y, \mathbf{u}_0 \in \mathbf{H}$. A quadruple $\{\mathbf{u}, p, \phi, \mu\}$ is called a weak solution of problem (1.1)–(1.10) if it satisfies*

$$\mathbf{u} \in L^\infty(0, T; \mathbf{H}), \quad \mathbf{u}_t \in L^{\frac{4}{3}}(0, T; \mathbf{H}') \quad (2.4)$$

$$\phi \in L^\infty(0, T; Y) \cap L^4(0, T; L^\infty(\Omega)), \quad \partial_t \phi \in L^2(0, T; Y'), \quad (2.5)$$

$$\mu \in L^2(0, T; Y), \quad p \in L^{\frac{4}{3}}(0, T; M), \quad (2.6)$$

and there hold, $\forall \{\mathbf{v}, q, v, \varphi\} \in \mathbf{X} \times M \times Y \times Y$ and $t \in (0, T)$ a.e.

$$\frac{ReDa}{\chi} \langle \partial_t \mathbf{u}, \mathbf{v} \rangle + (\alpha(\phi) \mathbf{u}, \mathbf{v}) - (p, \nabla \cdot \mathbf{v}) + \frac{\epsilon^{-1}}{We^*} (\phi \nabla \mu, \mathbf{v}) + (\nabla \cdot \mathbf{u}, q) = 0, \quad (2.7)$$

$$\chi \langle \partial_t \phi, v \rangle - (\phi \mathbf{u}, \nabla v) + \frac{1}{Pe} (M(\phi) \nabla \mu, \nabla v) = 0, \quad (2.8)$$

$$(\mu, \varphi) - (\phi^3 - \phi, \varphi) - \epsilon^2 (\nabla \phi, \nabla \varphi) = 0, \quad (2.9)$$

with initial condition $\mathbf{u}|_{t=0} = \mathbf{u}_0, \phi|_{t=0} = \phi_0$.

The regularity requirements in (2.4)–(2.6) are suggested by the energy law Eq. (1.11). The existence of such a weak solution can be established similarly as [9] (see also [38, 18, 26]).

B. The fully discrete numerical schemes

Let N be a positive integer and $0 = t_0 < t_1 < \dots < t_N = T$ be a uniform partition of $[0, T]$. Denote by $k := t_n - t_{n-1}$, $n = 1, 2, \dots, N$, the time step-size.

Let \mathcal{T}_h be a regular, quasi-uniform triangulation of the domain Ω in 2D with mesh size h . We introduce the continuous mixed finite element approximations of \mathbf{X} and M based on \mathcal{T}_h , denoted by \mathbf{X}_h and M_h respectively. Furthermore, we assume \mathbf{X}_h and M_h satisfy the inf-sup condition for the divergence operator, i.e.,

$$\exists C > 0, \quad \sup_{\mathbf{v}_h \in \mathbf{X}_h} \frac{(\nabla \cdot \mathbf{v}_h, q_h)}{\|\mathbf{v}_h\|_{H^1}} \geq C \|q_h\|_{L^2}, \quad \forall q_h \in M_h.$$

In \mathbf{X}_h , we assume the following inverse inequality holds [22]

$$\exists C > 0, \quad \|\mathbf{v}_h\|_{L^4} \leq C \frac{1}{h^{1/2}} \|\mathbf{v}_h\|_{L^2}, \quad \forall \mathbf{v}_h \in \mathbf{X}_h. \quad (2.10)$$

Commonly used finite element spaces for \mathbf{X}_h and M_h include the Taylor-Hood finite element space and the Mini finite element space, cf. [10]. Similarly, we define Y_h a continuous finite element approximation of Y . Typical examples of Y_h include

$$Y_h = \{v_h \in C(\bar{\Omega}) | v_h|_K \in P_r(K), \forall K \in \mathcal{T}_h\},$$

where $P_r(K)$ is the space of polynomials of degree less than or equal to r on the triangle K .

We now introduce our first fully discrete numerical scheme, denoted by **(N1)** hereafter: find $\{\mathbf{u}_h^{n+1}, p_h^{n+1}, \phi_h^{n+1}, \mu_h^{n+1}\} \in \mathbf{X}_h \times M_h \times Y_h \times Y_h$ such that

$$\begin{aligned} & \frac{ReDa}{\chi} \left(\frac{\mathbf{u}_h^{n+1} - \mathbf{u}_h^n}{k}, \mathbf{v}_h \right) + (\alpha(\phi_h^n) \mathbf{u}_h^{n+1}, \mathbf{v}_h) - (p_h^{n+1}, \nabla \cdot \mathbf{v}_h) \\ & + \frac{\epsilon^{-1}}{We^*} (\phi_h^n \nabla \mu_h^{n+1}, \mathbf{v}_h) + (\nabla \cdot \mathbf{u}_h^{n+1}, q_h) = 0, \quad \forall \mathbf{v}_h \in \mathbf{X}_h, q_h \in M_h, \end{aligned} \quad (2.11)$$

$$\chi \left(\frac{\phi_h^{n+1} - \phi_h^n}{k}, v_h \right) - (\phi_h^n \mathbf{u}_h^n, \nabla v_h) + \frac{1}{Pe} (m(\phi_h^n) \nabla \mu_h^{n+1}, \nabla v_h) = 0, \quad \forall v_h \in Y_h, \quad (2.12)$$

$$(\mu_h^{n+1}, \varphi_h) - ((\phi_h^{n+1})^3 - \phi_h^n, \varphi_h) - \epsilon^2 (\nabla \phi_h^{n+1}, \nabla \varphi_h) = 0, \quad \forall \varphi_h \in Y_h, \quad (2.13)$$

with initial condition $\mathbf{u}_h^0 = \mathbf{u}_{0h}, \phi_h^0 = \phi_{0h}$, where $\mathbf{u}_{0h}, \phi_{0h}$ are the projection of \mathbf{u}_0, ϕ_0 in \mathbf{X}_h, Y_h , respectively.

Note that the velocity in the Cahn-Hilliard equation (2.12) is treated explicitly in time. Thus the Darcy equation (2.11) is completely decoupled from the rest of the equations. One can solve the system sequentially: first solve the Cahn-Hilliard Eqs. (2.12) and (2.13) for ϕ_h^{n+1} and μ_h^{n+1} by, for instance, Newton's method; then solve the linear Darcy equation (2.11) for \mathbf{u}_h^{n+1} and p_h^{n+1} . In comparison to the coupled scheme, i.e., treating velocity implicitly \mathbf{u}_h^{n+1} in Eq. (2.12), scheme **(N1)** is much more efficient, cf. the efficiency test in section III.

Next, following the operator-splitting strategy introduced in [29], we propose another decoupled numerical scheme **(N2)** as follows:

find $\{\mathbf{u}_h^{n+1}, p_h^{n+1}, \phi_h^{n+1}, \mu_h^{n+1}\} \in \mathbf{X}_h \times M_h \times Y_h \times Y_h$ such that

$$\begin{aligned} & \frac{ReDa}{\chi} \left(\frac{\mathbf{u}_h^{n+1} - \mathbf{u}_h^n}{k}, \mathbf{v}_h \right) + (\alpha(\phi_h^n) \mathbf{u}_h^{n+1}, \mathbf{v}_h) - (p_h^{n+1}, \nabla \cdot \mathbf{v}_h) \\ & + \frac{\epsilon^{-1}}{We^*} (\phi_h^n \nabla \mu_h^{n+1}, \mathbf{v}_h) + (\nabla \cdot \mathbf{u}_h^{n+1}, q_h) = 0, \quad \forall \mathbf{v}_h \in \mathbf{X}_h, q_h \in M_h, \end{aligned} \quad (2.14)$$

$$\chi \left(\frac{\phi_h^{n+1} - \phi_h^n}{k}, v_h \right) - (\phi_h^n \bar{\mathbf{u}}_h^{n+1}, \nabla v_h) + \frac{1}{Pe} (m(\phi_h^n) \nabla \mu_h^{n+1}, \nabla v_h) = 0, \quad \forall v_h \in Y_h, \quad (2.15)$$

$$(\mu_h^{n+1}, \varphi_h) - ((\phi_h^{n+1})^3 - \phi_h^n, \varphi_h) - \epsilon^2 (\nabla \phi_h^{n+1}, \nabla \varphi_h) = 0, \quad \forall \varphi_h \in Y_h, \quad (2.16)$$

with the intermediate velocity $\bar{\mathbf{u}}_h^{n+1}$ defined as

$$\frac{ReDa}{\chi} \frac{\bar{\mathbf{u}}_h^{n+1} - \mathbf{u}_h^n}{k} + \frac{\epsilon^{-1}}{We^*} \phi_h^n \nabla \mu_h^{n+1} = 0. \quad (2.17)$$

We note that the intermediate velocity $\bar{\mathbf{u}}_h^{n+1}$ never appears in the real computation. Indeed, upon substitution (Eq. (2.17)), we see that the only unknown variables in Eq. (2.15) and Eq. (2.16) are $\phi_h^{n+1}, \mu_h^{n+1}$. Thus the Cahn-Hilliard system (Eqs. (2.15) and (2.16)) is completely decoupled from the Darcy equation (2.14). Also, note that formally $\bar{\mathbf{u}}_h^{n+1}$ is a first order approximation of \mathbf{u}_h^n . Therefore we expect scheme (N2) to be a first order scheme for the Cahn-Hilliard-Darcy system.

Remark. *We remark that the pairing $Y_h \times Y_h$ of equal order finite element spaces is a natural choice for ϕ_h and μ_h . Recall also that the Cahn-Hilliard equation is a fourth order equation, upon substitution of the definition of the chemical potential. Eqns. (2.12) and (2.13) are thus a mixed finite element formulation for solving the Cahn-Hilliard equation. The equal order finite element spaces $Y_h \times Y_h$ is a stable pair for the biharmonic operator (cf. [4]) in the sense that there holds the inf-sup condition*

$$\sup_{\phi_h \in Y_h} \frac{(\nabla \phi_h, \nabla \varphi_h)}{\|\phi_h\|_{H^1}} \geq c \|\varphi_h\|_{H^1}, \quad \forall \varphi_h \in Y_h \cap L_0^2(\Omega),$$

where $L_0^2(\Omega)$ is the subspace of $L^2(\Omega)$ with mean zero. The equivalence of the two spaces seems also necessary for higher-order stability estimates which are keys to establish optimal error estimates, cf. Remark 2.4 of [7].

C. Stability of the fully discrete schemes

In this subsection, we study the stability of the decoupled numerical schemes (N1) and (N2). We will show that scheme (N1) (Eqs. (2.11)-(2.13)) is conditionally energy-stable with a time step-size constraint, whereas the scheme (N2) (Eqs. (2.14)-(2.13)) is unconditionally stable. Without ambiguity, we denote by (f, g) the L^2 inner product between functions f and g .

First, we show that the fully discrete scheme (N1) satisfies an energy law under a mild CFL-like condition. We define a discrete analog of the energy functional (1.12) as follows

$$E^n = ReDa \int_{\Omega} \frac{1}{2\chi} |\mathbf{u}_h^n|^2 dx + \frac{1}{We^*} \int_{\Omega} \chi \left[\frac{1}{\epsilon} F(\phi_h^n) + \frac{\epsilon}{2} |\nabla \phi_h^n|^2 \right] dx. \quad (2.18)$$

Theorem 2.1. *At each time step, for any mesh parameters k, h and any $\epsilon > 0$, there exists a unique solution $\{\mathbf{u}_h^{n+1}, p_h^{n+1}, \phi_h^{n+1}, \mu_h^{n+1}\}$ to the scheme (N1) Eqns. (2.11)–(2.13). Moreover, if the following time step constraint is satisfied*

$$k \leq C \frac{ReDa\epsilon We^* m_1}{\chi^{\frac{1}{2}} Pe (8\epsilon We^* E^0 + 2\chi|\Omega|)^{\frac{1}{2}}} h, \quad (2.19)$$

the solution of the scheme (N1) satisfies a discrete energy law

$$\begin{aligned} \frac{E^{n+1} - E^n}{k} &\leq -\|\sqrt{\alpha(\phi_h^n)} \mathbf{u}_h^{n+1}\|_{L^2}^2 - \frac{\epsilon^{-1}}{2We^*Pe} \|\sqrt{m(\phi_h^k)} \nabla \mu_h^{n+1}\|_{L^2}^2 \\ &\quad - \frac{\chi\epsilon}{2We^*k} \|\nabla(\phi_h^{n+1} - \phi_h^n)\|_{L^2}^2. \end{aligned} \quad (2.20)$$

Proof. The unique solvability of Eqns. (2.11)–(2.13) can be established easily thanks to the decoupling and the convex-splitting treatment of the chemical potential equation. Here we highlight the ideas in the proof and refer to the appropriate references. Given ϕ_h^n, \mathbf{u}_h^n , Eqns. (2.12)–(2.13) amount to a first-order convex-splitting discretization of the Cahn-Hilliard equation with a known forcing term. Thus the unique solvability of the Cahn-Hilliard part follows from a variational argument by exploiting the convexity in the design and the gradient flow structure of the system, cf. [22, 39]. Once μ_h^{n+1} is known, Eq. (2.11) is a mixed finite element approximation of the Darcy equation. Its unique solvability is guaranteed by the inf-sup compatibility between \mathbf{X}_h and M_h , cf. [10]. We point out that the unique solvability can also be established via a monotonicity argument, cf. [17, 18].

We proceed to show that the energy law (2.20) is valid under the time step constraint (2.19). Testing Eq. (2.11) with $\mathbf{v}_h = \mathbf{u}_h^{n+1}$ and $q_h = p_h^{n+1}$, and utilizing the identity $a(a-b) = \frac{1}{2}[a^2 - b^2 + (a-b)^2]$, one obtains

$$\begin{aligned} &\frac{ReDa}{2\chi k} [\|\mathbf{u}_h^{n+1}\|_{L^2}^2 - \|\mathbf{u}_h^n\|_{L^2}^2 + \|\mathbf{u}_h^{n+1} - \mathbf{u}_h^n\|_{L^2}^2] + \|\sqrt{\alpha(\phi_h^n)} \mathbf{u}_h^{n+1}\|_{L^2}^2 \\ &+ \frac{\epsilon^{-1}}{We^*} (\phi_h^n \nabla \mu_h^{n+1}, \mathbf{u}_h^{n+1}) = 0. \end{aligned} \quad (2.21)$$

Next, taking the test function $v_h = \mu_h^{n+1}$ in Eq. (2.12) gives

$$\chi \left(\frac{\phi_h^{n+1} - \phi_h^n}{k}, \mu_h^{n+1} \right) - (\phi_h^n \mathbf{u}_h^n, \nabla \mu_h^{n+1}) + \frac{1}{Pe} \|\sqrt{m(\phi_h^n)} \nabla \mu_h^{n+1}\|_{L^2}^2 = 0. \quad (2.22)$$

Finally, we test Eq. (2.13) with $\varphi_h = -\frac{\phi_h^{n+1} - \phi_h^n}{k}$. Recall the following inequality associated with the first order convex-splitting of F [31]

$$F(\phi_h^{n+1}) - F(\phi_h^n) \leq [(\phi_h^{n+1})^3 - \phi_h^n][\phi_h^{n+1} - \phi_h^n].$$

We conclude that

$$\begin{aligned} & -\frac{1}{k}(\mu_h^{n+1}, \phi_h^{n+1} - \phi_h^n) + \frac{1}{k}(F(\phi_h^{n+1}) - F(\phi_h^n), 1) \\ & + \frac{\epsilon^2}{2k}[\|\nabla\phi_h^{n+1}\|_{L^2}^2 - \|\nabla\phi_h^n\|_{L^2}^2 + \|\nabla(\phi_h^{n+1} - \phi_h^n)\|_{L^2}^2] \leq 0. \end{aligned} \quad (2.23)$$

Multiplying the inequality (2.23) with χ and adding the result with Eq. (2.22), one has

$$\begin{aligned} & \frac{\chi}{k}(F(\phi_h^{n+1}) - F(\phi_h^n), 1) + \frac{\chi\epsilon^2}{2k}[\|\nabla\phi_h^{n+1}\|_{L^2}^2 - \|\nabla\phi_h^n\|_{L^2}^2] - (\phi_h^n \mathbf{u}_h^{n+1}, \nabla\mu_h^{n+1}) \\ & \leq -\frac{1}{Pe}\|\sqrt{m(\phi_h^n)}\nabla\mu_h^{n+1}\|_{L^2}^2 - \frac{\chi\epsilon^2}{2k}\|\nabla(\phi_h^{n+1} - \phi_h^n)\|_{L^2}^2. \end{aligned} \quad (2.24)$$

We next add Eq. (2.21) and inequality (2.24) scaled by $\frac{\epsilon^{-1}}{We^*}$ to obtain

$$\begin{aligned} & \frac{ReDa}{2\chi k}[\|\mathbf{u}_h^{n+1}\|_{L^2}^2 - \|\mathbf{u}_h^n\|_{L^2}^2 + \|\mathbf{u}_h^{n+1} - \mathbf{u}_h^n\|_{L^2}^2] + \frac{\chi\epsilon^{-1}}{kWe^*}(F(\phi_h^{n+1}) - F(\phi_h^n), 1) \\ & + \frac{\chi\epsilon}{2We^*k}[\|\nabla\phi_h^{n+1}\|_{L^2}^2 - \|\nabla\phi_h^n\|_{L^2}^2] \leq -\frac{\epsilon^{-1}}{We^*Pe}\|\sqrt{m(\phi_h^n)}\nabla\mu_h^{n+1}\|_{L^2}^2 \\ & - \frac{\chi\epsilon}{2We^*k}\|\nabla(\phi_h^{n+1} - \phi_h^n)\|_{L^2}^2 - \|\sqrt{\alpha(\phi_h^n)}\mathbf{u}_h^{n+1}\|_{L^2}^2 - \frac{\epsilon^{-1}}{We^*}(\phi_h^n \nabla\mu_h^{n+1}, [\mathbf{u}_h^{n+1} - \mathbf{u}_h^n]). \end{aligned} \quad (2.25)$$

We now control the last term in (2.25) as follows (cf. [22] for a similar argument)

$$\begin{aligned} & \left| \frac{\epsilon^{-1}}{We^*}(\phi_h^n \nabla\mu_h^{n+1}, [\mathbf{u}_h^{n+1} - \mathbf{u}_h^n]) \right| \\ & \leq \frac{\epsilon^{-1}}{We^*}\|\phi_h^n\|_{L^4}\|\mathbf{u}_h^{n+1} - \mathbf{u}_h^n\|_{L^4}\|\nabla\mu_h^{n+1}\|_{L^2} \\ & \leq \frac{\epsilon^{-1}}{We^*\sqrt{m_1}}\|\phi_h^n\|_{L^4}\|\mathbf{u}_h^{n+1} - \mathbf{u}_h^n\|_{L^4}\|\sqrt{m(\phi_h^n)}\nabla\mu_h^{n+1}\|_{L^2}, \quad \text{cf. (1.5)} \\ & \leq \frac{\epsilon^{-1}Pe}{2We^*m_1}\|\phi_h^n\|_{L^4}^2\|\mathbf{u}_h^{n+1} - \mathbf{u}_h^n\|_{L^4}^2 + \frac{\epsilon^{-1}}{2We^*Pe}\|\sqrt{m(\phi_h^n)}\nabla\mu_h^{n+1}\|_{L^2}^2 \\ & \leq C\frac{\epsilon^{-1}Pe}{2hWe^*m_1}\|\phi_h^n\|_{L^4}^2\|\mathbf{u}_h^{n+1} - \mathbf{u}_h^n\|_{L^2}^2 + \frac{\epsilon^{-1}}{2We^*Pe}\|\sqrt{m(\phi_h^n)}\nabla\mu_h^{n+1}\|_{L^2}^2, \end{aligned}$$

where the last inequality follows from the inverse inequality (2.10). The quantity $\|\phi_h^n\|_{L^4}^2$ can be bounded in terms of the total energy E^n . Notice that

$$\int_{\Omega} (\phi_h^n)^4 dx \leq 2 \int_{\Omega} \{[(\phi_h^n)^2 - 1]^2 + 1\} dx \leq 8 \int_{\Omega} F(\phi_h^n) + 2|\Omega|.$$

It follows from the definition of E^n in (2.18) that

$$\|\phi_h^n\|_{L^4}^2 \leq (8\epsilon We^* E^n / \chi + 2|\Omega|)^{\frac{1}{2}}.$$

Assuming $E^n \leq E^0$ for the time being, one can write the above inequality as

$$\|\phi_h^n\|_{L^4}^2 \leq (8\epsilon We^* E^0 / \chi + 2|\Omega|)^{\frac{1}{2}}. \quad (2.26)$$

Thus if the following condition is satisfied

$$k \leq C \frac{ReDa\epsilon We^* m_1}{\chi^{\frac{1}{2}} Pe (8\epsilon We^* E^0 + 2\chi|\Omega|)^{\frac{1}{2}}} h,$$

one has

$$\left| \frac{\epsilon^{-1}}{We^*} (\phi_h^n \nabla \mu_h^{n+1}, [\mathbf{u}_h^{n+1} - \mathbf{u}_h^n]) \right| \leq \frac{ReDa}{2\chi k} \|\mathbf{u}_h^{n+1} - \mathbf{u}_h^n\|_{L^2}^2 + \frac{\epsilon^{-1}}{2We^* Pe} \|\sqrt{m(\phi_h^n)} \nabla \mu_h^{n+1}\|_{L^2}^2. \quad (2.27)$$

Taking into account of inequality (2.27), one derives from inequality (2.25) the following modified energy law

$$\begin{aligned} & \frac{ReDa}{2\chi k} [\|\mathbf{u}_h^{n+1}\|_{L^2}^2 - \|\mathbf{u}_h^n\|_{L^2}^2] + \frac{\chi\epsilon^{-1}}{kWe^*} (F(\phi_h^{n+1}) - F(\phi_h^n), 1) \\ & + \frac{\chi\epsilon}{2We^* k} [\|\nabla \phi_h^{n+1}\|_{L^2}^2 - \|\nabla \phi_h^n\|_{L^2}^2] \leq -\frac{\epsilon^{-1}}{2We^* Pe} \|\sqrt{m(\phi_h^n)} \nabla \mu_h^{n+1}\|_{L^2}^2 \\ & - \frac{\chi\epsilon}{2We^* k} \|\nabla(\phi_h^{n+1} - \phi_h^n)\|_{L^2}^2 - \|\sqrt{\alpha(\phi_h^n)} \mathbf{u}_h^{n+1}\|_{L^2}^2. \end{aligned} \quad (2.28)$$

In particular, it follows that $E^{n+1} \leq E^n$. Thus an induction argument concludes the proof. ■

Remark. *Explicit time stepping for velocity in the Cahn-Hilliard equation as in scheme (N1) is a natural and common practice for the numerical simulation of Cahn-Hilliard fluid models, cf. [31]. It decouples the computation of Cahn-Hilliard equation and fluid equations, thus reducing the computational cost. The stability of such a time*

stepping scheme is investigated in [22] in the context of Cahn-Hilliard-Navier-Stokes fluid model where a similar time step constraint as (2.19) is established. Another CFL-like condition is suggested numerically in [1] by considering the solvability of the numerical scheme at a single time step. The result is for Cahn-Hilliard-Navier-Stokes system, and is independent of the spatial resolution.

Now we show that the numerical scheme (N2) is unconditionally energy-stable.

Theorem 2.2. *At each time step, for any mesh parameters k, h and any $\epsilon > 0$, there exists a unique solution $\{\mathbf{u}_h^{n+1}, p_h^{n+1}, \phi_h^{n+1}, \mu_h^{n+1}\}$ to the scheme (N2) Eqns. (2.14)–(2.16). Moreover, the solution of the scheme (N2) satisfies a discrete energy law*

$$\begin{aligned} \frac{E^{n+1} - E^n}{k} &\leq -\|\sqrt{\alpha(\phi_h^n)}\mathbf{u}_h^{n+1}\|_{L^2}^2 - \frac{\epsilon^{-1}}{We^*Pe} \|\sqrt{m(\phi_h^n)}\nabla\mu_h^{n+1}\|_{L^2}^2 \\ &\quad - \frac{\chi\epsilon}{2We^*k} \|\nabla(\phi_h^{n+1} - \phi_h^n)\|_{L^2}^2 - \frac{ReDa}{2\chi k} (\|\bar{\mathbf{u}}_h^{n+1} - \mathbf{u}_h^n\|_{L^2}^2 + \|\mathbf{u}_h^{n+1} - \bar{\mathbf{u}}_h^{n+1}\|_{L^2}^2), \end{aligned} \quad (2.29)$$

where the intermediate velocity $\bar{\mathbf{u}}_h^{n+1}$ is defined in Eq. (2.17), and the discrete energy law is given by (2.18).

Proof. The solvability of the scheme (N2) can be established in the same way as the scheme (N1). Indeed, by using the definition of the intermediate velocity (2.17), Eq. (2.15) can be rewritten in the form of Eq. (2.12) with a modified mobility function $\tilde{m}(\phi_h^n) := m(\phi_h^n) + \frac{\epsilon^{-1}k\chi Pe}{We^*ReDa}(\phi_h^n)^2$.

For the stability, we note that the treatment of the Cahn-Hilliard system (Eqns. (2.15) and (2.16)) are the same as in the proof of Theorem 2.1, cf. Eqns. (2.22) and (2.23). One can obtain (compare to Eq. (2.24))

$$\begin{aligned} &\frac{\chi}{We^*k} \left\{ \frac{1}{\epsilon} (F(\phi_h^{n+1}) - F(\phi_h^n), 1) + \frac{\epsilon}{2} [\|\nabla\phi_h^{n+1}\|_{L^2}^2 - \|\nabla\phi_h^n\|_{L^2}^2] \right\} - \frac{\epsilon^{-1}}{We^*} (\phi_h^n \bar{\mathbf{u}}_h^{n+1}, \nabla\mu_h^{n+1}) \\ &\leq -\frac{\epsilon^{-1}}{PeWe^*} \|\sqrt{m(\phi_h^n)}\nabla\mu_h^{n+1}\|_{L^2}^2 - \frac{\chi\epsilon}{2We^*k} \|\nabla(\phi_h^{n+1} - \phi_h^n)\|_{L^2}^2. \end{aligned} \quad (2.30)$$

Next, we multiply Eq. (2.17) by $\bar{\mathbf{u}}_h^{n+1}$ and integrate

$$\frac{ReDa}{2\chi k} [\|\bar{\mathbf{u}}_h^{n+1}\|_{L^2}^2 - \|\mathbf{u}_h^n\|_{L^2}^2 + \|\bar{\mathbf{u}}_h^{n+1} - \mathbf{u}_h^n\|_{L^2}^2] + \frac{\epsilon^{-1}}{We^*} (\phi_h^n \nabla\mu_h^{n+1}, \bar{\mathbf{u}}_h^{n+1}) = 0. \quad (2.31)$$

In view of the definition of the intermediate velocity (2.17), the Darcy Eq.(2.14) can be reformulated as $\forall \mathbf{v}_h \in \mathbf{X}_h, q_h \in M_h$,

$$\frac{ReDa}{\chi} \left(\frac{\mathbf{u}_h^{n+1} - \bar{\mathbf{u}}_h^n}{k}, \mathbf{v}_h \right) + (\alpha(\phi_h^n) \mathbf{u}_h^{n+1}, \mathbf{v}_h) - (p_h^{n+1}, \nabla \cdot \mathbf{v}_h) + (\nabla \cdot \mathbf{u}_h^{n+1}, q_h) = 0.$$

Taking the test function $\mathbf{v}_h = \mathbf{u}_h^{n+1}$ in the above equation, one has

$$\frac{ReDa}{2\chi k} [\|\mathbf{u}_h^{n+1}\|_{L^2}^2 - \|\bar{\mathbf{u}}_h^{n+1}\|_{L^2}^2 + \|\mathbf{u}_h^{n+1} - \bar{\mathbf{u}}_h^{n+1}\|_{L^2}^2] + \|\sqrt{\alpha(\phi_h^n)} \mathbf{u}_h^{n+1}\|_{L^2}^2 = 0. \quad (2.32)$$

The energy law (2.29) now follows from adding up Eqs. (2.30), (2.31) and (2.32). ■

III. NUMERICAL EXPERIMENTS

In this section, we report some numerical results to show the accuracy and efficiency of the numerical scheme **(N1)** (Eqs. (2.11)–(2.13)) and the scheme **(N2)** (Eqs. (2.14)–(2.16)). Throughout, we take Y_h to be the P1 or P2 finite element function space. For \mathbf{X}_h and M_h , the celebrated Taylor-Hood finite elements (P2–P1) and Mini finite elements (P1b–P1) will be used. We solve the nonlinear equations (2.12)–(2.13) and (2.15)–(2.16), respectively, by the classical Newton’s method. All the numerical tests are performed using the free software FreeFem++ [19].

A. Convergence test

In our first numerical test, we verify the first order convergence in time for both the scheme **(N1)** and the scheme **(N2)**. For convenience, we take all the parameters in the CHD system (1.1)–(1.4) to be unity and work on the unit square $\Omega = [0, 1] \times [0, 1]$. We proceed by the method of manufactured solutions. Specifically, we assume that there are forcing terms in Eqs. (1.1), (1.3) and (1.4) such that the exact solutions of the system are as follows

$$\begin{aligned} \mathbf{u} &= \left(-\sin^2(\pi x) \sin(2\pi y) \cos(t), \sin^2(\pi y) \sin(2\pi x) \cos(t) \right), \\ p &= \cos(t) \left(xy - \frac{1}{4} \right), \\ \phi &= \cos(t) \cos(\pi x) \cos(\pi y), \\ \mu &= \sin(t) \cos(\pi x) \cos(\pi y). \end{aligned}$$

We use P2–P2 finite elements for ϕ_h^{n+1} and μ_h^{n+1} , P2–P1 pair for \mathbf{u}_h^{n+1} and p_h^{n+1} . The spatial resolution is fixed at $h = 0.01\sqrt{2}$ such that the spatial error is negligible compared to temporal error in the following calculation. We successively decrease the time step-size k . We compute the solution up to a final time $T = 0.5$ and record the error measured in L^2 norm. An error estimate of the form $\mathcal{O}(h^3) + \mathcal{O}(k)$ is anticipated for \mathbf{u}, ϕ, μ , whereas the one for pressure is $\mathcal{O}(h^2) + \mathcal{O}(k)$, cf. [7] for similar results. The first order convergence in time is clearly shown in Fig. 1. We mention that we have also carried out Cauchy convergence tests by simultaneously decreasing temporal and spatial step-size. Our results (not included here) also verify the first order in time convergence rate.

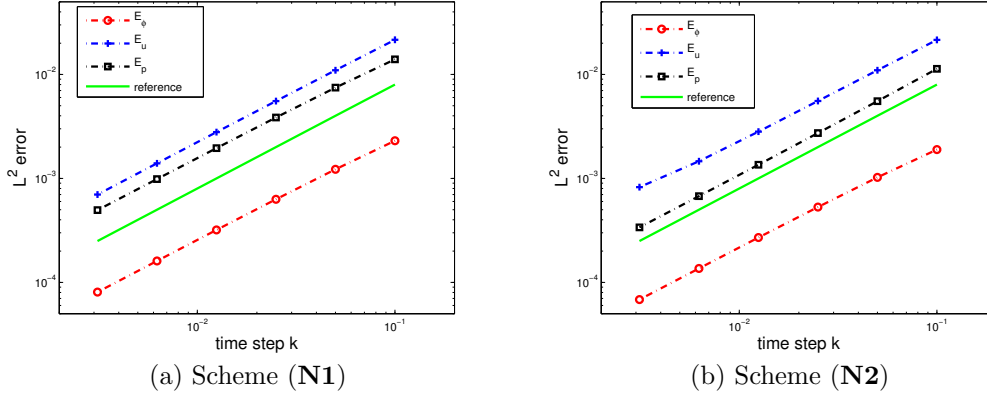


FIG. 1. Temporal convergence test: L^2 error of the velocity \mathbf{u} , the pressure p , and the order parameter ϕ as a function of time step k . The solid green line is the reference line $e = 0.08k$. The final time is $T = 0.5$. $h = 0.01\sqrt{2}$. P2–P2 is used for ϕ and μ , P2–P1 is used for \mathbf{u} and p . The other parameters are set to be unity.

B. Stability test

In this subsection, we study and compare the stability of the scheme (N1) and scheme (N2) by numerical experiments. The numerical test is the standard shape relaxation driven by surface tension that is studied by many authors [23, 39, 17, 34]. We consider a binary fluid of square shape at rest initially (cf. Fig. 2). The surface tension effect will drive the square to become a circular shape in a way such that the total energy decreases

to a minimal. Thus this numerical test is a good choice for the study of the capabilities of energy-law preserving (stability) of the schemes.

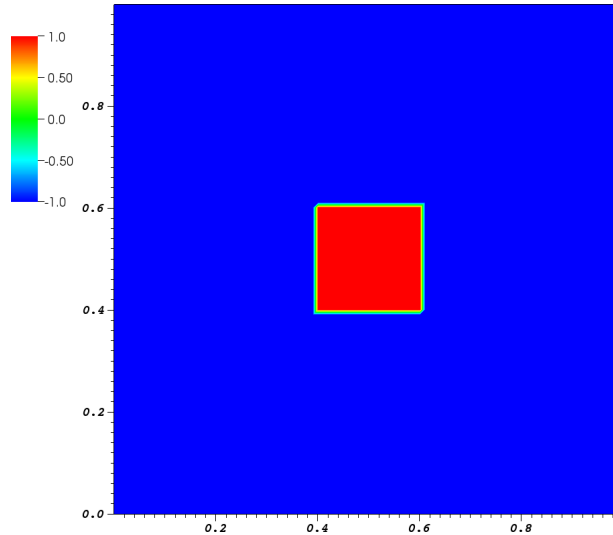


FIG. 2. The initial shape of the order parameter for simulations of shape relaxation.

To better address the multiple spatial scales of the problem, we explore the adaptive mesh refinement of FreeFem++ (cf. [19]) which uses a variable metric/Delaunay automatic meshing algorithm. Specifically, we adapt the mesh according to the Hessian of the order parameter such that approximately four grid cells are located across the diffuse interface.

The problem parameters are set as follows: $\epsilon = 0.01$, $We^* = 1$, $Pe = \frac{1}{\epsilon}$, $\chi = 0.5$, $\frac{ReDa}{\chi} = 0.1$, $\alpha(\phi) = 10$, and $m(\phi) = 1$. This set-up of the problem corresponds to an extreme case in the sense that the theoretical time step constraint in (2.19) for the scheme (N1) is at the order of 10^{-6} . We plot the evolution of the total energy in time associated with (N1) and (N2), respectively, using different time step-sizes. From Fig. 3 (a), we see that the discrete energy is non-increasing for the scheme (N1) with $k = 2e - 4$. However, when $k = 3.5e - 4$, the discrete total energy of (N1) starts increasing very quickly (cf. Fig. 3 (b)). In contrast, the discrete energy for (N2) appears to be non-increasing, even at $k = 0.01$.

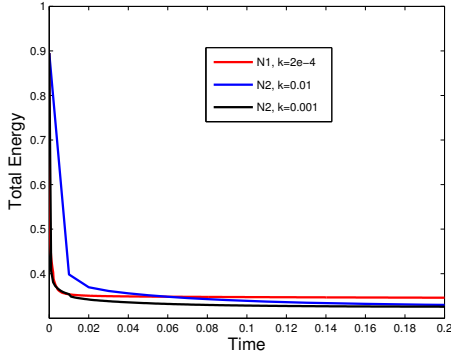
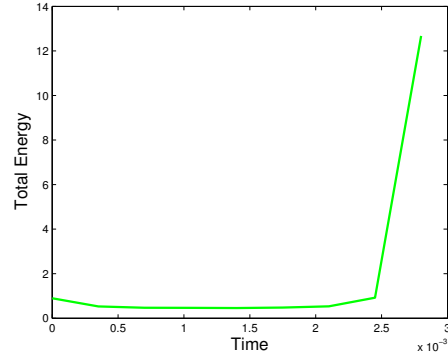
(a) stable cases, **N1** and **N2**(b) unstable case, **N1**, $k = 3.5e - 4$

FIG. 3. Stability test: time evolution of the total energy of Scheme (**N1**) and (**N2**) at different time step-sizes.

Two snapshots of the relaxed shape at time $t = 0.002$ are shown in Fig. 4. The scheme (**N2**) well captures the relaxation of the square shape using relatively large time step $k = 0.01$, whereas oscillations and instabilities start to grow around the corners of the square when computed by the scheme (**N1**) with $k = 3.5e - 4$. We remark that the

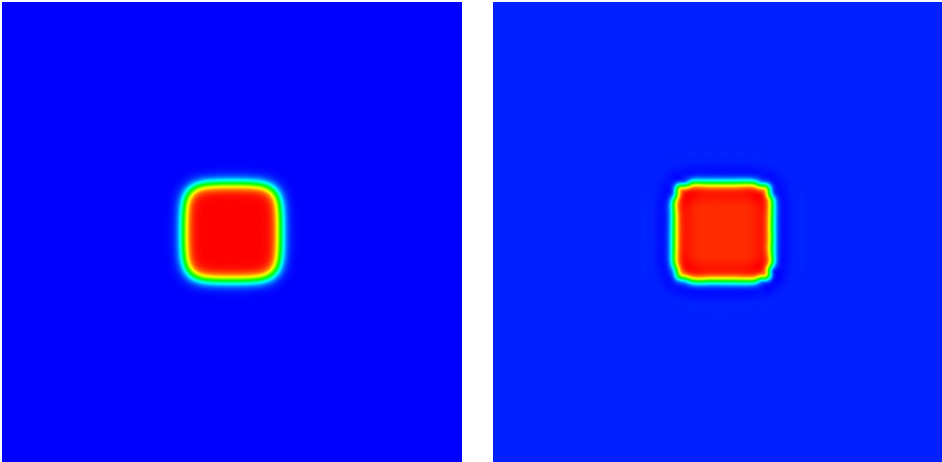
(a) **N2**, $k = 0.01$ (b) **N1**, $k = 3.5e - 4$

FIG. 4. Snapshots of the shape at $t = 0.002$.

time step constraint (2.19) for (**N1**) is only a sufficient condition for the validation of a discrete energy law. In this numerical example, it is clear that much larger time step is

allowed (10^{-6} vs. 10^{-4}). Also, the result here seems to echo with part of the numerical findings in [1], i.e., the time step constraint is independent of spatial resolution.

C. Efficiency test

Here we compare the efficiency of the scheme (N1) and the scheme (N2) in terms of CPU time. We will also compare their performance relative to a fully coupled unconditionally stable scheme which is a variant of the scheme (N1) with the velocity treated implicitly in Eq. (2.12). Since our schemes are relatively efficient, this set of numerical tests are carried out in a Dell Inspiron 15-7537 laptop with the following specifications: Intel Core i7 4510U (quad CPUs, dual core, 2.0 GHZ); 16G RAM. The test problem is the same as the one in convergence test, i.e., all parameters are unity. We keep a record of the CPU time in seconds for each scheme running up to $T = 0.5$ at the same time step. The spatial resolution is set as $h = 0.02\sqrt{2}$. $P2$ finite elements are used for \mathbf{u}, ϕ, μ and $P1$ is used for pressure p . The nonlinear systems are solved using Newton’s iteration method with the same tolerance $1e - 8$.

The averaged computation time with different time step-sizes is summarized in Table I. In comparison, we see that the decoupled schemes are three to four times faster than the fully coupled scheme, not to mention the extra memory cost for the coupled scheme. Also, the scheme (N2) is slightly faster than the scheme (N1), possibly due to the better stability of N2 considering virtually the same implementation of both schemes. Note that the computational time does not scale with k , since we are solving nonlinear systems using iterative methods.

TABLE I. Efficiency test: actual CPU time in seconds for each scheme with various time steps computed to $T = 0.5$. The problem parameters are all unity.

<i>scheme</i>	$k = 0.1$	$k = 0.05$	$k = 0.025$	$k = 0.0125$	$k = 0.00625$	$k = 0.003125$
Coupled	166.80	362.86	697.40	777.47	1562.98	3137.42
N1	41.18	76.69	158.38	200.11	383.46	769.99
N2	38.72	74.74	157.09	198.94	381.66	769.12

D. Interface pinchoff

One of the main advantages of the diffuse interface models is that they can capture topological transitions of the fluids interface (in the sense of sharp interface model) smoothly, cf. [27]. In this experiment, we demonstrate the effectiveness of our numerical schemes in the simulation of binary fluids with topological interface changes. Due to the unconditional stability, we will mainly use scheme **(N2)**.

We consider a situation where a light fluid layer initially sandwiched by two heavy fluid layers in a square domain $\Omega = [0, 2\pi] \times [0, 2\pi]$ (cf. Fig. 5). For simplicity, we assume that the density variance of two fluids is small so that a Boussinesq approximation can be employed. Specifically, we take the background density as 1.0 and add the following buoyancy term to the Darcy equation in (1.1)

$$-b(\phi)\hat{\mathbf{y}} = -G(\rho(\phi) - \bar{\rho})\hat{\mathbf{y}} = -G\frac{\rho_1 - \rho_2}{2}(\phi - \bar{\phi})\hat{\mathbf{y}} := -\lambda(\phi - \bar{\phi})\hat{\mathbf{y}},$$

where $\hat{\mathbf{y}}$ is the unit vector pointing upwards ($\hat{\mathbf{y}} = (0, 1)$), G is the gravitational constant, $\rho(\phi) = \frac{1+\phi}{2}\rho_1 + \frac{1-\phi}{2}\rho_2$ with $\rho_2 \approx \rho_1 = 1.0$, $\bar{\rho}$ is the spatially averaged density, $\bar{\phi}$ is the spatially averaged order parameter, and $\lambda = G\frac{\rho_1 - \rho_2}{2}$. Introducing two flat interfaces with small perturbations

$$y_1(x) = \pi - (0.5 + 0.1 \cos(x)), \quad y_2(x) = \pi + (0.5 + 0.1 \cos(x)),$$

then the initial condition for the phase field variable is defined as

$$\phi_0 = \tanh\left(\frac{y - y_1(x)}{\sqrt{2}\epsilon}\right) \tanh\left(\frac{y - y_2(x)}{\sqrt{2}\epsilon}\right).$$

In the simulation, boundary conditions (1.8)–(1.10) are imposed. A similar experiment has been carried out in [25] with periodic boundary condition, see also [14].

In the simulation shown in Fig. 6, we take $\epsilon = 0.05$, $Pe = 20$, $We^* = 4$, $m(\phi) = 1.0$, $\lambda = 2.946$, $\alpha(\phi) = \frac{1+\phi}{2}1.2 + \frac{1-\phi}{2}6$, $\chi = 0.5$ and $\frac{ReDa}{\chi} = 0.01$. For time stepsize, we choose $k = 0.001$. In space, P1b–P1 finite elements are used for \mathbf{u} and p , and P1–P1 finite elements are used for ϕ and μ . We adapt the mesh every five time steps according to the Hessian of the order parameter such that at least 6 grid cells are located across the diffuse interface.

Contour plots in gray scale of the order parameter are shown in Fig. 6. In the language of sharp interface models, the upper interface is unstably stratified. The heavy

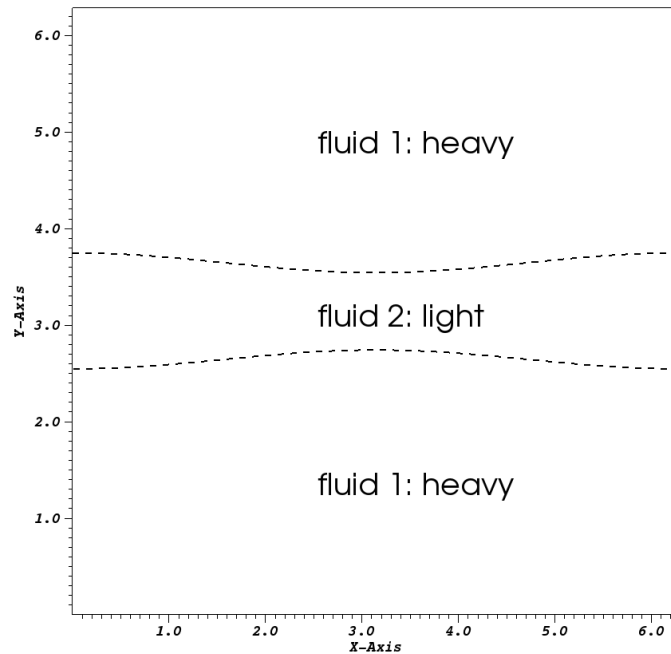


FIG. 5. The initial configuration of the phase field variable. $\epsilon = 0.05$. The dash lines are the zero contour of the interfaces.

fluid layer penetrates the light fluid layer, eventually causes the pinchoff of the light fluid layer. The break-up event is captured by our numerical algorithm. The effectiveness of the empirical adaptive mesh refinement can be observed from Fig. 7 as well where one can not differentiate the triangles in the interfacial region due to the dense density there.

IV. CONCLUSION

We propose and compare two decoupled energy-law preserving numerical schemes for solving the Cahn-Hilliard-Darcy system modelling two-phase incompressible flows in porous medium or a Hele-Shaw cell. In the first scheme, explicit treatment of the velocity in the Cahn-Hilliard equation is utilized to decouple the computation. The scheme

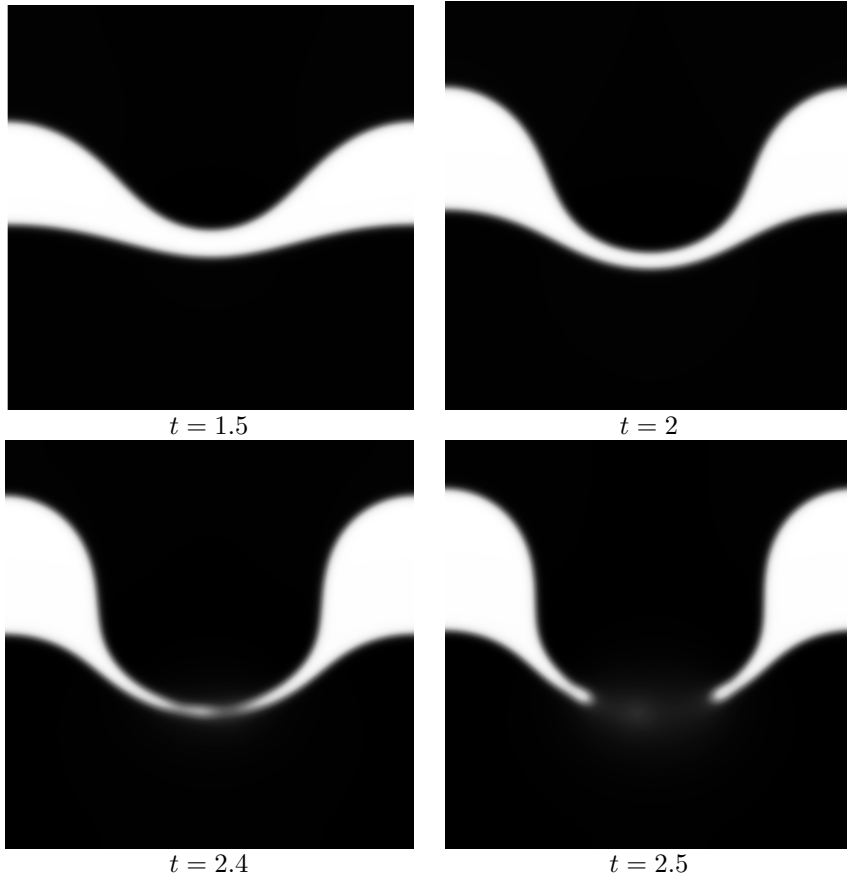


FIG. 6. Interface pinchoff due to buoyancy: contour plots of the order parameter in gray scale. $\epsilon = 0.05$, $Pe = 20$, $We^* = 4$, $m(\phi) = 1.0$, $\lambda = 2.946$, $k = 0.001$, $\chi = 0.5$, $\frac{ReDa}{\chi} = 0.01$ and $\alpha(\phi) = \frac{1+\phi}{2}1.2 + \frac{1-\phi}{2}6$.

is shown to be uniquely solvable and satisfy a discrete energy law with a time step constraint. The second numerical scheme employs an intermediate velocity (fractional stepping) in the computation of Cahn-Hilliard equation. Moreover, we show that the scheme satisfies a discrete energy law without any time constraint. We provide numerical evidence that both schemes work properly. The schemes present in the paper can be potentially generalized to solve other diffuse interface models for groundwater flow, for instance, the Cahn-Hilliard-Stokes-Darcy system [15].

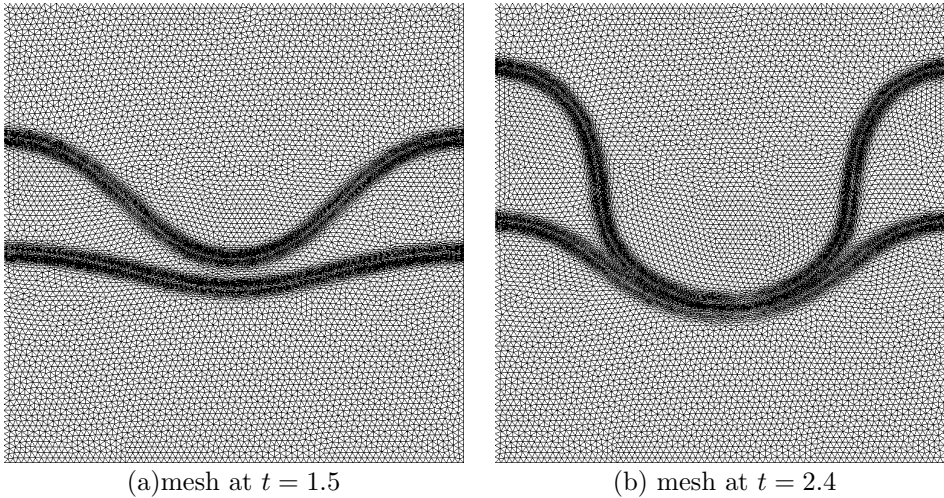


FIG. 7. Adaptive mesh refinement: meshes associated with the computation at $t = 1.5$ and $t = 2.4$, respectively.

Another decoupling strategy by combining fractional stepping and pressure stabilization is proposed in [14] for solving a Cahn-Hilliard-Hele-Shaw system. The scheme is shown to satisfy a modified discrete energy law as well. Though our schemes in this paper and the scheme in [14] are shown to be efficient, they are only first order accurate in time. The ideas in the design of decoupled energy-law abiding numerical schemes do not seem to have a direct generalization to higher order schemes. The design of higher order accurate, decoupled, energy-law preserving schemes requires further investigation.

ACKNOWLEDGEMENTS

This work is supported in part by a grant from the NSF (DMS1312701), and a multidisciplinary support grant from the Florida State University.

REFERENCES

1. S. ALAND, *Time integration for diffuse interface models for two-phase flow*, J. Comput.

- Phys., 262 (2014), pp. 58–71.
2. D. M. ANDERSON, G. B. MCFADDEN, AND A. A. WHEELER, *Diffuse-interface methods in fluid mechanics*, in Annual review of fluid mechanics, Vol. 30, vol. 30 of Annu. Rev. Fluid Mech., Annual Reviews, Palo Alto, CA, 1998, pp. 139–165.
 3. J. BEAR, *Dynamics of fluids in porous media*, Courier Dover Publications, Sep 1, 1988.
 4. F. BREZZI AND M. FORTIN, *Mixed and hybrid finite element methods*, vol. 15 of Springer Series in Computational Mathematics, Springer-Verlag, New York, 1991.
 5. N. CHEMETOV AND W. NEVES, *The generalized Buckley-Leverett system: solvability*, Arch. Ration. Mech. Anal., 208 (2013), pp. 1–24.
 6. C. COLLINS, J. SHEN, AND S. M. WISE, *An efficient, energy stable scheme for the Cahn-Hilliard-Brinkman system*, Commun. Comput. Phys., 13 (2013), pp. 929–957.
 7. A. E. DIEGEL, X. H. FENG, AND S. M. WISE, *Analysis of a mixed finite element method for a Cahn-Hilliard-Darcy-Stokes system*, SIAM J. Numer. Anal., 53 (2015), pp. 127–152.
 8. D. J. EYRE, *Unconditionally gradient stable time marching the Cahn-Hilliard equation*, in Computational and mathematical models of microstructural evolution (San Francisco, CA, 1998), vol. 529 of Mater. Res. Soc. Sympos. Proc., MRS, Warrendale, PA, 1998, pp. 39–46.
 9. X. FENG AND S. WISE, *Analysis of a Darcy-Cahn-Hilliard diffuse interface model for the Hele-Shaw flow and its fully discrete finite element approximation*, SIAM J. Numer. Anal., 50 (2012), pp. 1320–1343.
 10. V. GIRAULT AND P.-A. RAVIART, *Finite element methods for Navier-Stokes equations*, vol. 5 of Springer Series in Computational Mathematics, Springer-Verlag, Berlin, 1986. Theory and algorithms.
 11. G. GRÜN, *On convergent schemes for diffuse interface models for two-phase flow of incompressible fluids with general mass densities*, SIAM J. Numer. Anal., 51 (2013), pp. 3036–3061.
 12. R. GUO, Y. XIA, AND Y. XU, *An efficient fully-discrete local discontinuous Galerkin method for the Cahn-Hilliard-Hele-Shaw system*, J. Comput. Phys., 264 (2014), pp. 23–40.
 13. Z. GUO, P. LIN, AND J. S. LOWENGRUB, *A numerical method for the quasi-incompressible Cahn-Hilliard-Navier-Stokes equations for variable density flows with a discrete energy law*, J. Comput. Phys., 276 (2014), pp. 486–507.

14. D. HAN, *A decoupled unconditionally stable numerical scheme for the Cahn-Hilliard-Hele-Shaw system*, Journal of Scientific Computing, (2015), pp. 1–20.
15. D. HAN, D. SUN, AND X. WANG, *Two-phase flows in karstic geometry*, Mathematical Methods in the Applied Sciences, 37 (2014), pp. 3048–3063.
16. D. HAN AND X. WANG, *Initial-boundary layer associated with the nonlinear Darcy-Brinkman system*, J. Differential Equations, 256 (2014), pp. 609–639.
17. D. HAN AND X. WANG, *A second order in time, uniquely solvable, unconditionally stable numerical scheme for Cahn-Hilliard-Navier-Stokes equation*, J. Comput. Phys., 290 (2015), pp. 139–156.
18. D. HAN, X. WANG, AND H. WU, *Existence and uniqueness of global weak solutions to a Cahn-Hilliard-Stokes-Darcy system for two phase incompressible flows in karstic geometry*, J. Differential Equations, 257 (2014), pp. 3887–3933.
19. F. HECHT, *New development in freefem++*, J. Numer. Math., 20 (2012), pp. 251–265.
20. Z. HU, S. M. WISE, C. WANG, AND J. S. LOWENGRUB, *Stable and efficient finite-difference nonlinear-multigrid schemes for the phase field crystal equation*, J. Comput. Phys., 228 (2009), pp. 5323–5339.
21. J. JIANG, H. WU, AND S. ZHENG, *Well-posedness and long-time behavior of a non-autonomous cahnhilliardarcy system with mass source modeling tumor growth*, Journal of Differential Equations, (2015), pp. –.
22. D. KAY, V. STYLES, AND R. WELFORD, *Finite element approximation of a Cahn-Hilliard-Navier-Stokes system*, Interfaces Free Bound., 10 (2008), pp. 15–43.
23. D. KAY AND R. WELFORD, *A multigrid finite element solver for the Cahn-Hilliard equation*, J. Comput. Phys., 212 (2006), pp. 288–304.
24. H.-G. LEE, J. S. LOWENGRUB, AND J. GOODMAN, *Modeling pinchoff and reconnection in a Hele-Shaw cell. I. The models and their calibration*, Phys. Fluids, 14 (2002), pp. 492–513.
25. H.-G. LEE, J. S. LOWENGRUB, AND J. GOODMAN, *Modeling pinchoff and reconnection in a Hele-Shaw cell. II. Analysis and simulation in the nonlinear regime*, Phys. Fluids, 14 (2002), pp. 514–545.

26. J. LOWENGRUB, E. TITI, AND K. ZHAO, *Analysis of a mixture model of tumor growth*, European J. Appl. Math., 24 (2013), pp. 691–734.
27. J. LOWENGRUB AND L. TRUSKINOVSKY, *Quasi-incompressible Cahn-Hilliard fluids and topological transitions*, R. Soc. Lond. Proc. Ser. A Math. Phys. Eng. Sci., 454 (1998), pp. 2617–2654.
28. F. MAGALETTI, F. PICANO, M. CHINAPPI, L. MARINO, AND C. M. CASCIOLA, *The sharp-interface limit of the Cahn-Hilliard-Navier-Stokes model for binary fluids*, Journal of Fluid Mechanics, 714 (2013), pp. 95–126.
29. S. MINJEAUD, *An unconditionally stable uncoupled scheme for a triphasic Cahn-Hilliard/Navier-Stokes model*, Numer. Methods Partial Differential Equations, 29 (2013), pp. 584–618.
30. D. A. NIELD AND A. BEJAN, *Convection in porous media*, Springer-Verlag, New York, second ed., 1999.
31. J. SHEN, *Modeling and numerical approximation of two-phase incompressible flows by a phase-field approach*, in Multiscale modeling and analysis for materials simulation, vol. 22 of Lect. Notes Ser. Inst. Math. Sci. Natl. Univ. Singap., World Sci. Publ., Hackensack, NJ, 2012, pp. 147–195.
32. J. SHEN, C. WANG, X. WANG, AND S. M. WISE, *Second-order convex splitting schemes for gradient flows with Ehrlich-Schwoebel type energy: application to thin film epitaxy*, SIAM J. Numer. Anal., 50 (2012), pp. 105–125.
33. J. SHEN AND X. YANG, *A phase-field model and its numerical approximation for two-phase incompressible flows with different densities and viscosities*, SIAM J. Sci. Comput., 32 (2010), pp. 1159–1179.
34. J. SHEN AND X. YANG, *Decoupled, energy stable schemes for phase-field models of two-phase incompressible flows*, SIAM Journal on Numerical Analysis, 53 (2015), pp. 279–296.
35. J. SHEN, X. YANG, AND H. YU, *Efficient energy stable numerical schemes for a phase field moving contact line model*, Journal of Computational Physics, 284 (2015), pp. 617 – 630.
36. C. WANG, X. WANG, AND S. M. WISE, *Unconditionally stable schemes for equations of thin film epitaxy*, Discrete Contin. Dyn. Syst., 28 (2010), pp. 405–423.

37. X. WANG AND H. WU, *Long-time behavior for the Hele-Shaw-Cahn-Hilliard system*, *Asymptot. Anal.*, 78 (2012), pp. 217–245.
38. X. WANG AND Z. ZHANG, *Well-posedness of the Hele-Shaw-Cahn-Hilliard system*, *Ann. Inst. H. Poincaré Anal. Non Linéaire*, 30 (2013), pp. 367–384.
39. S. M. WISE, *Unconditionally stable finite difference, nonlinear multigrid simulation of the Cahn-Hilliard-Hele-Shaw system of equations*, *J. Sci. Comput.*, 44 (2010), pp. 38–68.